

Molecular Wire Electronic State Crossing Driven by Applied Voltage

Gabin Treboux*

National Institute for Advanced Interdisciplinary Research, 1-1-4 Higashi, Tsukuba-shi, Ibaraki 305-8562, Japan

Received: April 26, 2000; In Final Form: August 15, 2000

The effect of applying an external voltage to a molecular wire connecting two reservoirs of states is analyzed through the use of a Hubbard Hamiltonian which explicitly depends on the applied voltage. The Hamiltonian is solved using a method based on two-by-two rotations of molecular orbitals, which avoids divergence, and permits both ground and excited states to be obtained. The special case of a polyacene wire is studied in detail as a function of the wire length. It is shown that the energies of the ground and excited states of the wire cross as the voltage is increased. This crossing produces specific features in the current–voltage characteristic of the molecular wire.

Introduction

The potential for using single molecules¹ as basic components of electronic circuits is receiving an increasing amount of interest due to recent impressive experimental results^{2–4} and the development of theoretical tools for the design of molecular electronics is becoming of technological interest.^{5,6} Until recently, the current–voltage (I/V) characteristics of molecules have been modeled using the Landauer formalism,⁷ using a tight-binding Hamiltonian for the calculation of the molecular orbitals (MO) forming the conducting channels.^{8–11} The use of a tight-binding Hamiltonian is a major drawback since the effect of electron repulsion on the Hamiltonian solution is not included. This prevents as well the taking into account of the applied voltage.^{12,13} An appealing approach to overcome these limitations is the use of a Hubbard Hamiltonian depending explicitly on the applied voltage, as proposed recently by Mujica et al.⁵ While conserving the computational tractability of the entire model, this approach has revealed important insights on the effect of the applied voltage on molecular wire conductance.⁵ Using this approach, I studied the possibility of electronic state crossing in a molecular wire subjected to an external voltage. Due to the limitation involved in the approach, the result presented here should be considered as qualitative only. Nonetheless, more sophisticated models based on *ab initio* methodology have recently been proposed. It should be therefore possible, even if somewhat challenging in terms of computational resources, to address the effect presented in this article using such models in order to obtain more quantitative predictions.^{14–16}

On the basis of technological requirements, molecular wires are expected to conduct electric current at low voltages. Such an expectation can be translated, in terms of chemistry, by designing molecular wires having a delocalized wave function and a small energy gap between occupied and virtual MOs. Molecular candidates might therefore be selected among aromatic systems which have delocalized π orbitals. The energy gap between MOs can be tuned by the length of the molecular wire.⁶ Synthetic processes permitting the length control of the molecular wire are well understood and usually result in

molecular wires of high symmetry. Because of the difference in polarizability of MOs having different symmetries, the corresponding energy levels are modified differently as the applied voltage is increased and are therefore expected to cross for an experimentally realistic value of the applied voltage. To quantify this effect, both the ground state and the excited states must be computed as a function of the applied voltage. The complexity of the energy dependence on the applied voltage is illustrated for a series of polyacene molecules of increasing length (see Figure 1). The expected effect is observed and it produces specific features in the I/V characteristic of the molecular wire.

Conductance Model. I implemented the algorithm recently proposed by Mujica et al.^{17,18} for solving the general problem of electronic conduction between two reservoirs of states via a molecular wire. In this approach, the system consists of a molecule bridging two noninteracting reservoirs of states. The first atom of the molecule is connected to the left reservoir A and the last atom (N) to the right reservoir B (see Figure 1).

Using the T-matrix formalism of the scattering theory,^{19–21} the quantum conductance is derived as

$$g = \frac{2e^2}{\pi h} |G_{1N}|^2 \Delta_A(E_F) \Delta_B(E_F)$$

where G is Green's function of the Hamiltonian of the total system. The subscript $1N$ stands for the matrix element connecting atoms 1 and N . Δ is the reservoir spectral density defined through Newns chemisorption theory²² as

$$\Delta_K(E) = \begin{cases} \frac{\beta_K^2}{\gamma} \sqrt{1 - \left(\frac{E}{2\gamma}\right)^2}, & \left|\frac{E}{2\gamma}\right| < 1 \\ 0, & \text{otherwise} \end{cases}$$

where E is measured from the center of the reservoir energy band, and 4γ and β are, respectively, the reservoir bandwidth and the strength of the chemisorption coupling between the molecule and the reservoir.

The problem of finding the infinite dimensional Green's function matrix G_{1N} is mapped to an $N \times N$ problem using Lowdin's partitioning technique.^{23,24} The electronic Hubbard

* E-mail: gabin@nair.go.jp.

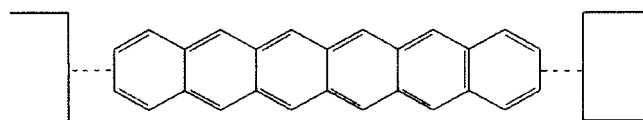


Figure 1. Schematic representation of a polyacene (6-acene) molecule connecting two reservoirs of states. The first atom of the molecule is connected to the left reservoir A and the last atom (N) to the right reservoir B. The dotted line represents the conduction axis.

Hamiltonian²⁵ of the wire is given by

$$H_M = \sum_{i,k} \alpha_{i,k} + \beta \sum_{i,j,k} a_{i,k}^\dagger a_{j,k} + \text{c. c.} + U \sum_i n_{i,up} n_{i,down}$$

Mujica et al. generalized the model for the case of finite voltage as the integral of the conductance between the Fermi levels of the two reservoirs:

$$J(V) = \frac{2e}{\pi\hbar} \int_{E_F - eV}^{E_F} dE \Delta_A(E) \Delta_B(E + eV) \times |G_{1N}(E, V)|^2$$

In this approach, Green's function depends explicitly on the voltage. Assuming that the electric potential between the reservoirs varies linearly with the distance, the diagonal element of the Hamiltonian α at the site k of the wire is given by $a_{i,k} \rightarrow a_{i,k} + V_k$ and the electric potential at the site k of the wire by $V_k = eV x_k/D$ where D is the distance between the two reservoirs, and x_k is the x distance of site k from the origin at the left reservoir.

Solution of the Hubbard Hamiltonian. In the approach presented in ref 5, the Hamiltonian is solved self-consistently using the Hartree–Fock approximation. Several sources of non convergence exist during the self-consistent procedure. The first one is due to the Hartree–Fock approximation. The procedure is known to diverge as soon as the Hubbard term exceeds twice the hopping integral ($U > 2\beta$).²⁶ To circumvent this problem, a method based on the second derivative of the energy must be used for larger values of the Hubbard term.²⁷ The second one is due to the occurrence of permutation between one or more virtual and occupied levels between successive iterations of the self-consistent procedure. This appears frequently for systems having a small energy gap between occupied and virtual MOs, i.e., for the systems relevant to molecular electronics. Artificial level shift is often used to circumvent such problems. The results obtained using this technique, nonetheless, are not a guarantee mathematically. I propose, instead, a procedure based on an earlier proposal by Rossi.²⁸ In this procedure the solution of the Hubbard Hamiltonian is obtained by successive two-by-two rotations of the MOs, each rotation angle obtained by solving the Brillouin theorem. The orbitals thus obtained still constitute a solution of the Hartree–Fock equation. Given a set of n occupied orthonormal MOs $\varphi_{i,o}$ and a set of m unoccupied orthonormal MOs $\varphi_{i,u}$ all the possible rotations of a single electron of the type

$$\varphi_{i,1} = \cos\theta \varphi_{i,0} + \sin\theta \varphi_{j,0}$$

$$\varphi_{j,1} = -\sin\theta \varphi_{i,0} + \cos\theta \varphi_{j,0}$$

are performed. The rotation angle θ is obtained analytically by applying the condition $\partial E / \partial \theta = 0$ where E is the energy of the system, which yields

$$\tan(2\theta) = 2\langle \varphi_i | H_M | \varphi_j \rangle / (\langle \varphi_i | H_M | \varphi_i \rangle - \langle \varphi_j | H_M | \varphi_j \rangle)$$

The process is iterated using the new set of MOs until all the

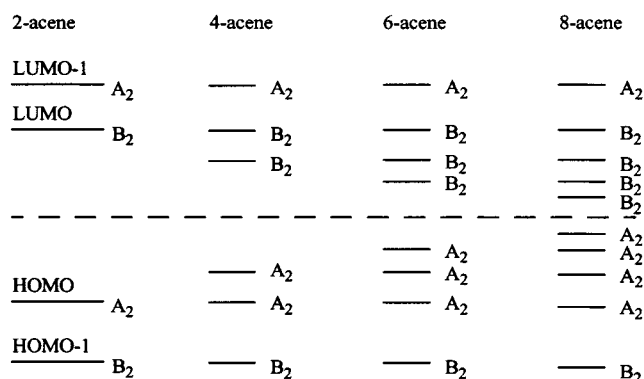


Figure 2. Schematic representation of the molecular level distribution for the polyacene molecules. The bias voltage is applied along the conduction axis (see Figure 1). The system is therefore studied under C_{2v} point group symmetry. The dotted line represents the Fermi level of the molecules, which is set to zero.

rotation angles are equal to zero. This method solves the non convergence problem associated with energy level permutation, since it relies, by construction, not on the energy level position but on the MO initial guess. In the present version of the program, a tight-binding Hamiltonian is used to form the initial guess. The crossing effect studied in the present article is based on the fact that ground and excited states have different symmetries. The single determinant wave function obtained by the Hartree–Fock procedure, therefore, must change symmetry when the voltage is varied. At the vicinity of the crossing voltage, the ground and excited states have almost identical energies and the Hartree–Fock procedure will usually terminate with a wave function which exhibits a symmetry-breaking artifact. This artifact is exempt from the procedure presented here, where, by construction, the symmetry of a given state is conserved for any value of applied voltage.

Results

Before discussing the dependence of the energy on the applied voltage, it is useful to review some symmetry properties of the MOs of a polyacene system. The application of the bias voltage reduces the symmetry of the molecules to the C_{2v} point group symmetry (see Figure 1). Considering the naphthalene molecule (2-acene), the highest occupied molecular orbital (HOMO) has A_2 symmetry and the lowest unoccupied molecular orbital (LUMO) has B_2 symmetry. In contrast, HOMO-1 and LUMO+1 have B_2 and A_2 symmetries, respectively (see Figure 2). Increasing the size of the molecule to tetracene (4-acene) leads to the appearance of a new unoccupied level of B_2 symmetry and a new occupied level of A_2 symmetry (see Figure 2). The same effect is obtained for every two additional benzene rings.

In Figure 3, the dependence of the energy of the ground state (full curve) and first excited state (dotted curve) of the tetracene system on the applied voltage is shown. A tight-binding Hamiltonian is used to compute the initial guess of the ground-state MOs, and an initial guess of the first excited state MOs is obtained by swapping HOMO with LUMO of the ground state MOs. At each voltage, the Hamiltonian is solved self-consistently using the two-by-two rotation procedure for both ground and excited states. No orthogonalization of the two states is necessary because of their different symmetries.

In Figure 4, the dependence of the energy of the ground state (full curve) and first excited state (dotted curve) of the octacene system on the applied voltage is shown. At zero bias voltage, the MOs are ordered as shown in Figure 2. Note that, as the system size increases the difference in energy between the

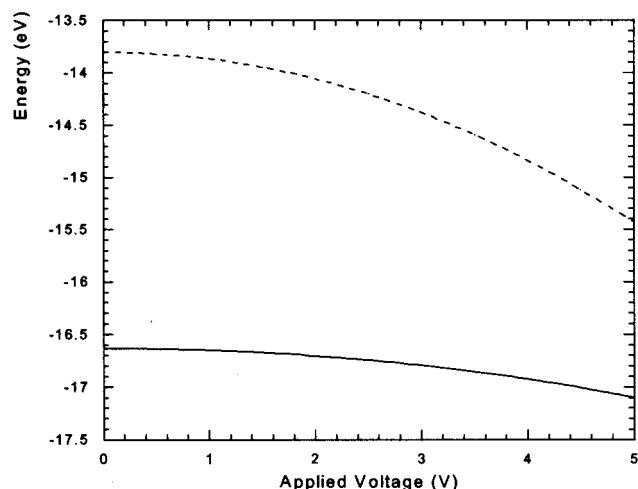


Figure 3. Energy dependence on the applied voltage of the ground state (full curve) and the first excited state (dotted curve) of the tetracene molecule. Parameters: $\beta = -2.4$ eV, $U = 2\beta$ (Hubbard Hamiltonian).

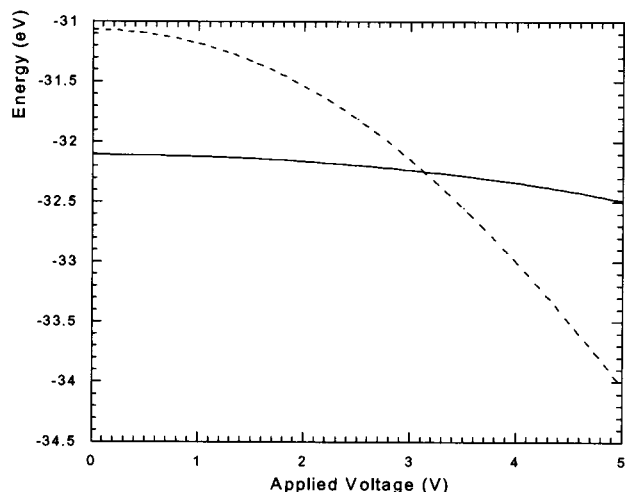


Figure 4. Energy dependence on the applied voltage of the ground state (full curve) and the first excited state (dotted curve) of the octacene molecule. Parameters: $\beta = -2.4$ eV, $U = 2\beta$ (Hubbard Hamiltonian). The crossing of the two states occurs at an applied voltage of 3.1 V.

ground state and the first excited state at zero voltage decreases. Because of the difference in polarizability of the MOs belonging to the two different symmetries, the corresponding energy levels are modified differently as the bias voltage is increased. This effect leads to the crossing of the ground and first excited states at an applied voltage of 3.1 V.

In Figure 5 the I/V characteristics for the ground (full curve) and the first excited (dotted curve) states of the octacene molecule are shown. The I/V characteristic for the ground state (full curve) is analyzed first. On application of a voltage with respect to the center of the band gap, initially no current flows from the left reservoir to the right reservoir, since all the energy levels of the wire are outside the integration window ($E_F, E_F - eV$). However, when the voltage is increased further, a step in the current is obtained. This step results from the HOMO and LUMO of the wire entering the integration window simultaneously; they enter simultaneously because both the algorithm and the Hamiltonian are electron-hole symmetric. Similarly, successive steps in the curve occur as the applied voltage increases and encompasses successively higher-energy MOs. The gradual decrease in current after each step is due to the voltage-induced localization of the MOs.⁵ The I/V characteristic for the first excited state (dotted curve) can be interpreted

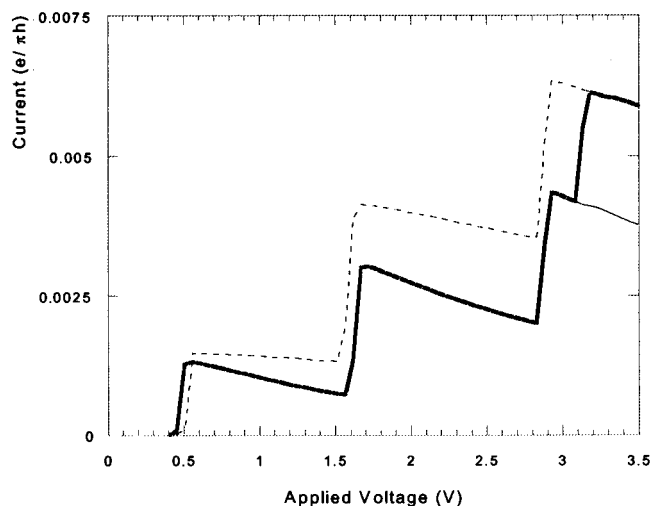


Figure 5. I/V characteristic of the octacene molecule (thick full curve), which coincides with the I/V characteristic of the ground state (thin full curve) from 0 to 3.1 V and of the first excited state (dotted curve) above 3.1 V. Parameters: $\beta = -2.4$ eV, $U = 2\beta$ (Hubbard Hamiltonian), $\beta_1 = \beta_n = 0.5$ eV, $\gamma = 10$ eV. The crossing of the two states occurs at an applied voltage of 3.1 V.

similarly. It is worth noting that because each MO of the excited state is different from the corresponding MO of the ground state, they enter the integration window at different applied voltages. The downward slope of the steps shows that the MOs of the excited state are less localized by the applied voltage than the corresponding MOs of the ground state. This results in a higher current passing through the wire in the case of the excited state. On the basis of the energy calculation, the I/V characteristic of octacene coincides with the full curve from 0 to 3.1 V and the dotted curve above 3.1 V (thick full curve). The crossing of ground and excited states leads to the appearance of a supplemental feature, i.e., a supplemental step in the I/V characteristics at the crossing voltage. This step is not related to a MO entering the integration window but is due to the difference in efficiency of the ground and excited states of sustaining the current.

It is possible to extend the method by taking into account the two states simultaneously through a multireference scheme which would give a more reliable I/V characteristic, particularly in the vicinity of the crossing of the two states. The details of this extension of the algorithm is postponed to the next article in this series.

Selection Rule

Increasing the size of the molecule increases the complexity of the energy dependence on the applied voltage. I therefore introduce a set of rules for selecting a priori the states which must be calculated, and analyze the MOs of the 16-acene molecule as an example. At zero bias voltage, the first class of states where HOMO and HOMO-1 are of symmetry A is defined. This class is labeled A-A. The ground state has class A-A. A second class of states labeled B-A is defined by swapping the HOMO with the LUMO of the ground state (excitation E_1 in Figure 7). The HOMO and LUMO have different symmetries, so they may cross as the bias voltage increases. The first excited state has class B-A and must be calculated. The excited state corresponding to excitation E_2 in Figure 7 also has class B-A, as does state E_3 . For any MO guess within a class, the two-by-two self-consistent procedure yields the same result. Therefore, the states E_2 and E_3 need not

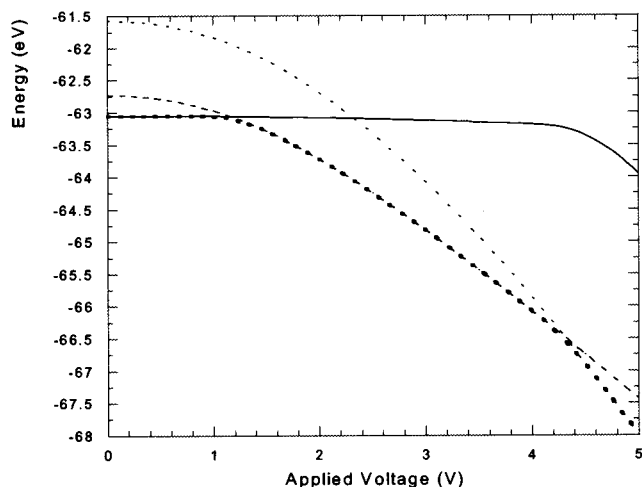


Figure 6. Energy dependence on the applied voltage of the states of symmetry A-A (full curve), A-B and B-B (dotted curves) of the 16-acene molecule. Parameters: $\beta = -2.4$ eV, $U = 2\beta$ (Hubbard Hamiltonian). The crossing of A-A and A-B occurs at an applied voltage of 1.2 V. The crossings of A-A and B-B, and A-B and B-B occur at applied voltages of 2.35 and 4.3 V, respectively. The thick dotted line represents the calculation without symmetry constraints. This state successively overlaps the states of symmetries A-A, A-B, and B-B and exhibits the phenomenon of symmetry-breaking of the Hartree-Fock wave function in the vicinity of applied voltages of 1.2 and 4.3 V.

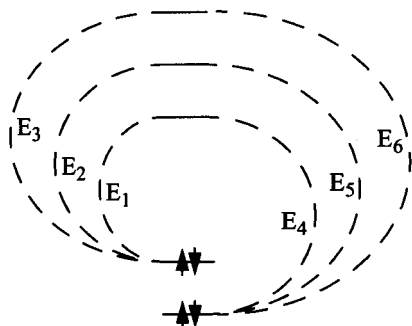


Figure 7. Schematic representation of all possible mono-excitations from the window [HOMO-1... LUMO+2] of MOs.

be considered. The next class of states to be considered is obtained by simultaneously swapping HOMO and HOMO-1 with LUMO+1 and LUMO, respectively, because their crossing is allowed by symmetry. Class B-B is thus obtained. A state of class B-B is formed, for example, by the excitation $E_2 + E_4$ in Figure 7. The energy dependence on the applied voltage of the three different symmetry states is shown in Figure 6. As the voltage is increased, a crossing of A-A and A-B indeed occurs, followed by a crossing of A-A and B-B, and then A-B and B-B. Different symmetries can be treated similarly to determine a priori the minimum set of determinants which must be calculated. This ensures that the lowest energy state of the system at any voltage is calculated, and gives a minimal set of determinants for performing further multireference expansion of the wave function.

Ab initio calculations were performed on the octacene molecule to verify the prediction obtained with the Hubbard Hamiltonian. The octacene ground and first singlet excited states were calculated within the B3LYP density functional formalism using CEP-31G basis sets.^{29,30} The geometry of the molecule was first optimized for both ground and first singlet excited states and calculations, at these geometries, were performed for selected values of an applied electric field. The electric field was applied along the conduction axis direction and was

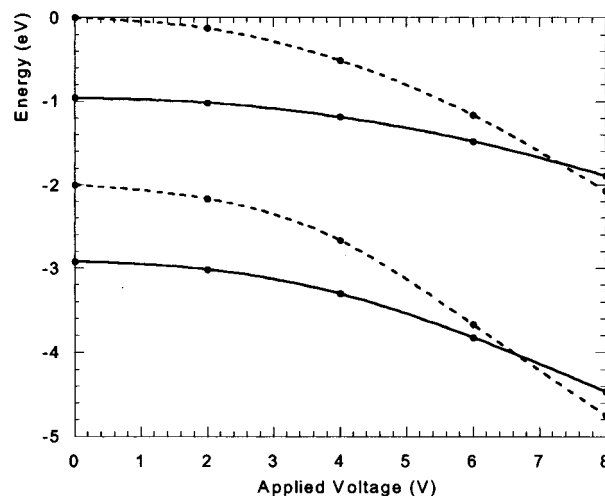


Figure 8. Energy dependence on the applied voltage of the ground state (upper full curve) and the first singlet excited state (upper dotted curve) of the octacene molecule. The crossing of the two states occurs at an applied voltage of 7.3 V. Energy dependence on the applied voltage of the ground state (lower full curve) and the first singlet excited state (lower dotted curve) of the thiol-substituted octacene molecule. The substitution of the two terminal hydrogen atoms by two thiol groups was performed at the left and right ends of the octacene molecule. The crossing of the two states occurs at an applied voltage of 6.7 V. The calculations were performed at selected applied voltages (dots) by the B3LYP density functional method using CEP-31G basis sets.^{29,30}

converted into applied voltage taking into account the length of the molecule. The result of the calculation is shown in Figure 8. The crossing of the two states occurs at an applied voltage of 7.3 V, to be compared with the value of 3.1 V found with the Hubbard Hamiltonian. The difference between these two values is indicative of the degree of overestimation of the orbital polarization by the Hubbard Hamiltonian. Due to the simplification involved in such Hamiltonian, the result could have been anticipated and underlines the qualitative nature of the model.

From an experimental point of view, the molecule must be chemically connected to electrodes. A practical procedure could be to substitute hydrogen atoms by thiol groups at the left and right ends of the molecule. The substitution of the two terminal hydrogen atoms by two thiol groups at the left and right ends of the octacene molecule has been considered as it conserves the symmetry of the system on the conduction axis. Ab initio calculations were performed for the thiol-substituted octacene molecule. The geometry of the substituted molecule was first optimized for both ground and first singlet excited states and energy calculations, at these geometries, were performed for selected values of an applied electric field. The result of the calculation is shown in Figure 8. The substitution of hydrogen by thiol groups does not qualitatively change the discussion presented in this article. Nonetheless, it changes significantly the energy dependence on the applied voltage. The crossing of the two states occurs at an applied voltage of 6.7 V and the polarization of the orbitals is increased. As pointed out by an anonymous referee, the energy level of the molecule could also be modified by the electrode interactions. This modification is likely to be significant and should also be taken into account in any quantitative discussion.

Conclusions

I have presented a quantum chemistry method that I have integrated into the algorithm recently proposed by Mujica et al.⁵ for solving the general problem of electronic conduction between two reservoirs of states via a molecular wire. This

method allows the study of both ground and excited states of the molecular wire at the Hubbard Hamiltonian level. Self-consistent solutions of the Hamiltonian were obtained by applying two-by-two rotations of the MOs, which avoids non convergence problems. A minimal set of states can be defined a priori to ensure that the lowest energy state of the molecular wire is found at any voltage. The special case of a polyacene wire was studied in detail as a function of the wire length. The energies of the different ground and excited states cross as the applied voltage is increased. These crossings were shown to produce steps in the I/V characteristic of the molecular wire. Such steps have a different nature from the successive steps previously analyzed in the I/V characteristic of molecular wires.⁵

Acknowledgment. The calculations were carried out at Silverbrook Research (Sydney, Australia) and at the AIST Tsukuba Advanced Computing Center.

References and Notes

- (1) Aviram, A.; Ratner, M. A. *Chem. Phys. Lett.* **1974**, 29, 277.
- (2) Reed, M. A.; Zhou, C.; Muller, C. J.; Burgin, T. P.; Tour, J. M. *Science* **1997**, 278, 252.
- (3) Tans, S. J.; Devoret, M. H.; Dai, H.; Thess, A.; Smalley, R. E.; Geerligs, L. J.; Dekker, C. *Nature* **1997**, 386, 474.
- (4) Collins, P. G.; Zettl, A.; Bando, H.; Thess, A.; Smalley, R. E. *Science* **1997**, 278, 5335.
- (5) Mujica, V.; Kemp, M.; Roitberg, A.; Ratner, M. A. *J. Chem. Phys.* **1996**, 104, 7296.
- (6) Magoga, M.; Joachim, C. *Phys. Rev. B* **1997**, 56, 4722.
- (7) Landauer, R. *IBM J. Res. Dev.* **1957**, 1, 223.
- (8) Chico, L.; Benedict, L. X.; Louie, S. G.; Cohen, M. L. *Phys. Rev. B* **1996**, 54, 2600.
- (9) Han, J.; Anantram, M. P.; Jaffe, R. L.; Kong, J.; Dai, H. *Phys. Rev. B* **1998**, 57, 14983.
- (10) Treboux, G. *J. Phys. Chem. B* **1999**, 103, 10378.
- (11) Igami, M.; Nakanishi, T.; Ando, T. *J. Phys. Soc. Jpn.* **1999**, 68, 716.
- (12) Lang, N. D. *Phys. Rev. B* **1995**, 52, 5335.
- (13) Farazdel, A.; Dupuis, M. *Phys. Rev. B* **1991**, 44, 3909.
- (14) Emberly, E. G.; Kirczenow, G. *Phys. Rev. B* **1998**, 58, 10911.
- (15) Yaliraki, S. N.; Roitberg, A. E.; Gonzalez, C.; Mujica, V.; Ratner, M. A. *J. Chem. Phys.* **1999**, 111, 6997.
- (16) Di ventra, M.; Pantelides, S. T.; Lang, N. D. *Phys. Rev. Lett.* **2000**, 84, 979.
- (17) Mujica, V.; Kemp, M.; Ratner, M. A. *J. Chem. Phys.* **1994**, 101, 6849.
- (18) Mujica, V.; Kemp, M.; Ratner, M. A. *J. Chem. Phys.* **1994**, 101, 6856.
- (19) Economou, E. N. *Green's Functions in Quantum Physics*; Springer: Berlin, 1990.
- (20) Taylor, J. R. *Scattering Theory*; Wiley: New York, 1972.
- (21) Davidov, A. S. *Quantum Mechanics*; NOE: Ann Arbor, 1966.
- (22) Newns, D. M. *Phys. Rev.* **1969**, 178, 1123.
- (23) Lowdin, P. O. *J. Math. Phys.* **1962**, 3, 969.
- (24) Evenson, J.; Karplus, M. *J. Chem. Phys.* **1992**, 96, 5272.
- (25) Hubbard, J. *Proc. R. Soc. London, Ser. A* **1963**, 276, 238.
- (26) Koutecky, J.; Bonacio, V. *J. Chem. Phys.* **1972**, 6, 171.
- (27) Broyden, C. G. *Mathematics of Computation* **1965**, 19, 577.
- (28) Rossi, M. *Theor. Chim. Acta* **1966**, 4, 30.
- (29) Frisch, M. J.; Trucks, G. W.; Schlegel, H. B.; Scuseria, G. E.; Robb, M. A.; Cheeseman, J. R.; Zakrzewski, V. G.; Montgomery, J. A.; Stratmann, R. E.; Burant, J. C.; Dapprich, S.; Millam, J. M.; Daniels, A. D.; Kudin, K. N.; Strain, M. C.; Farkas, O.; Tomasi, J.; Barone, V.; Cossi, M.; Cammi, R.; Mennucci, B.; Pomelli, C.; Adamo, C.; Clifford, S.; Ochterski, J.; Petersson, G. A.; Ayala, P. Y.; Cui, Q.; Morokuma, K.; Malick, D. K.; Rabuck, A. D.; Raghavachari, K.; Foresman, J. B.; Cioslowski, J.; Ortiz, J. V.; Stefanov, B. B.; Liu, G.; Liashenko, A.; Piskorz, P.; Komaromi, I.; Gomperts, R.; Martin, R. L.; Fox, D. J.; Keith, T.; Al-Laham, M. A.; Peng, C. Y.; Nanayakkara, A.; Gonzalez, C.; Challacombe, M.; Gill, P. M. W.; Johnson, B. G.; Chen, W.; Wong, M. W.; Andres, J. L.; Head-Gordon, M.; Replogle, E. S.; Pople, J. A. *Gaussian 98* (Revision A.3); Gaussian, Inc., Pittsburgh, PA, 1998.
- (30) Stevens, W.; Basch, H.; Krauss, J. *J. Chem. Phys.* **1984**, 81, 6026.